ChemComm

Rapid Thermally Assisted Donor-Acceptor Catenation

Albert C. Fahrenbach,[a] Karel J. Hartlieb,[a] Chi-Hau Sue,[a] Carson J. Bruns,[a] Gokhan Barin,[a] Subhadeep Basu,[a] Mark A. Olson,[b] Youssry Y. Botros,[a,c,d] Abdulaziz Bagabas,[a,d] Nezar H. Khdary,[a,d] and J. Fraser Stoddart[a]*

[a] *Department of Chemistry and Department of Materials Science and Engineering, Northwestern University, 2145 Sheridan Road, Evanston, IL, 60208-3113, United States*
[b] *Department of Physical & Environmental Sciences, Texas A&M University-Corpus Christi, 6300 Ocean Drive, Corpus Christi, Texas 78412-5774, United States*
[c] *Intel Labs, Building RNB-6-61, 2200 Mission College Blvd., Santa Clara, CA, 95054-1549, United States*
[d] *King Abdulaziz City for Science and Technology (KACST), P.O. Box 6086, Riyadh, 11442, Kingdom of Saudi Arabia*

*E-mail:stoddart@northwestern.edu

Electronic Supporting Information

Table of Contents

Experimental Section

1. General Methods

Starting materials and reagents were purchased from commercial suppliers and used as received. Compounds **S1**,[S1] **1a**,[S1] **1b**, [S2] **1c**, [S3] **1d,** [S4] 1,1-[1,4-phenylenebis(methylene)]-bis(4,4-bipyridinium) bis(hexafluorophosphate)[S5] (**2**·2PF_6) and the azido-bromomethyl-xylene derivative[S6] **4** were all synthesised according to procedures reported in the literature. All reactions were performed in dry solvents. Both analytical and preparative high performance liquid chromatography (HPLC) were performed on reversed phase-HPLC (RP-HPLC) instruments, using C_{18} columns and a binary solvent system, i.e., MeCN and H_2O with 0.1% (v / v) trifluoroacetic acid. All ^1H and ^{13}C NMR spectra were recorded on a Bruker Avance 500 MHz spectrometer at ambient temperature with working frequencies of 500 MHz or 125 MHz, respectively. The chemical shifts are listed in ppm on the δ scale relative to the signals corresponding to the residual non-deuterated solvents (CD_3CN: δ 1.94 ppm; $CDCl_3$: 7.26 ppm), and the coupling constants are recorded in Hertz (Hz). The following abbreviations were used to explain the multiplicities: s, singlet; d, doublet; t, triplet; b, broad peaks; m, multiplet or overlapping peaks. High resolution electrospray ionisation (HRESI) mass spectra were measured on a Micromass Q-TOF Ultima mass spectrometer. Matrix assisted laser desorption and ionisation – time of flight (MALDI-TOF) mass spectrometry was performed, using a Bruker Autoflex III instrument. Low resolution electrospray ionisation (LRESI) mass spectra were measured on an Agilent 1100 MSD tandem liquid chromatography mass spectrometer.

2. Synthetic Methods

General synthetic procedure for preparing compounds 5/6a-d: Macrocycle **1a**, **1b**, **1c, or 1d** (0.1 mmol) was mixed with a five-fold excess of 1,1-[1,4-phenylenebis-(methylene)]bis(4,4-bipyridinium) bis(hexafluorophosphate) **2**•2PF_6 (354 mg, 0.5 mmol) and 1,4-bis(bromomethyl)benzene **3** or its azide derivative **4** (0.5 mmol) in DMF (5 ml), and heated while stirring at 80˚C for 1 h. The solution was filtered and injected into preparative RP-HPLC (C_{18}; MeCN – H_2O / 0 – 50 % in 45 min, with 0.1% trifluoroacetic acid) for purification. The pure fractions collected were subjected to counterion exchange in order to afford products as crystalline solids.

5a•4PF_6: Purple solid (152.5mg, 88%). ^{1}H NMR (500 MHz, CD_3CN, 298 K) δ = 8.86 (b, 4H), 8.39 (b, 4H), 8.05 (b, 4H), 7.87 (b, 4H), 7.14 (m, 4H), 6.89 (b, 8H), 6.35 (d, J = 7.8 Hz, 2H), 6.06 (d, J = 7.8 Hz, 2H), 5.81 (t, J = 7.8 Hz, 2H), 5.72 (m, 8H), 4.21–3.70 (b, 32H), 2.26 (d, J = 7.8 Hz, 2H) ppm. HRMS (ESI) calcd for $C_{72}H_{76}F_{24}N_4O_{10}P_4$ [M – 2PF_6]$^{2+}$, m/z: 723.2422, found: 723.2449 [M – 2PF_6]$^{2+}$.

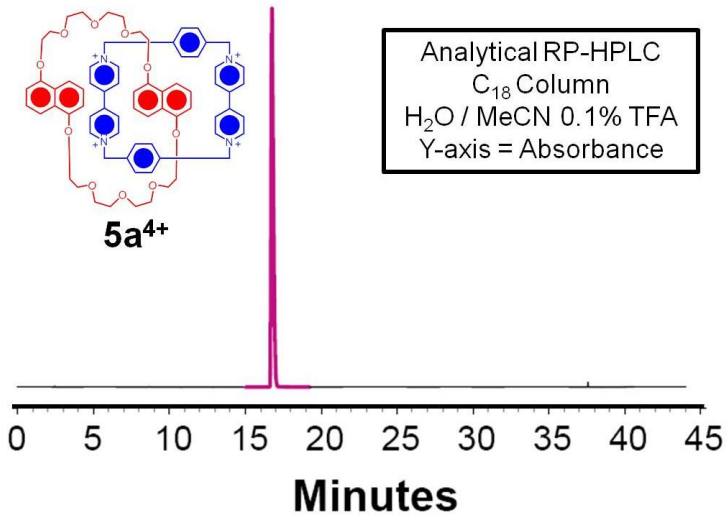

Figure S1. Analytical RP-HPLC of the pure catenane **5a**$^{4+}$; Abs @ 300 nm.

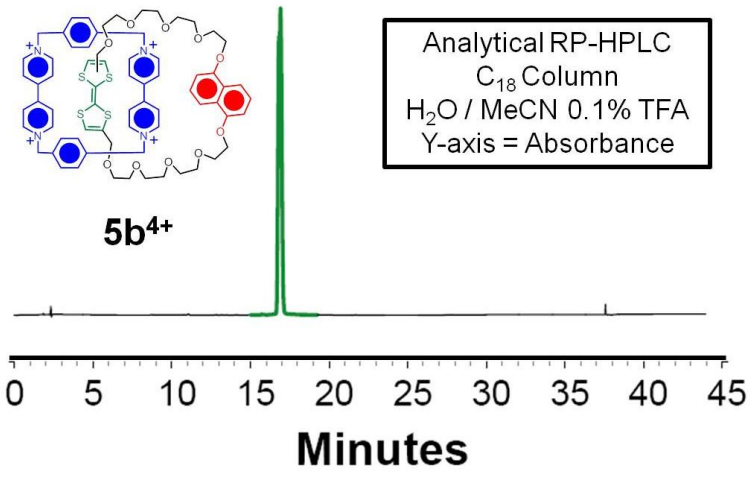

Figure S2. Analytical RP-HPLC of the pure catenane **5b**$^{4+}$; Abs @ 300 nm.

5b•4PF$_6$: Green solid (115 mg, 63%). ^{1}H NMR (500 MHz, CD_3CN, 298 K) δ =.8.91 (d, J = 6.7 Hz, 4H), 8.71 (d, J = 6.7 Hz, 4H), 7.61 (b, 8H), 7.45 (d, J = 6.3 Hz, 4H), 7.36 (m, 6H), 7.30 (t, J = 8.0 Hz, 2H), 6.71 (d, J = 8.0 Hz, 2H), 6.09 (s, 2H), 5.96 (m, 8H), 4.81 (s, 4H), 3.97–3.60 (b, 32H) ppm. HRMS (ESI) calcd for $C_{70}H_{76}F_{24}N_4O_{10}P_4S_4$ $[M - 2PF_6]^{2+}$, m/z: 775.1863, found: 775.1846 $[M - 2PF_6]^{2+}$.

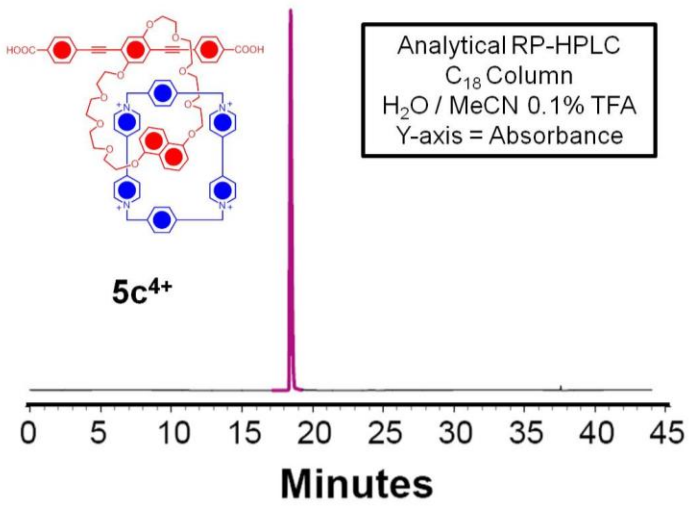

Figure S3. Analytical RP-HPLC of the pure catenane **5c**$^{4+}$; Abs @ 300 nm.

5c•4PF$_6$: Deep red solid (165 mg, 84%). ^{1}H NMR (500 MHz, CD_3SOCD_3, 298 K) δ = 9.08 (b, 8H), 8.09 (b, 12H), 7.54 (b, 12H), 6.39 (s, 2H), 6.03 (d, J = 7.5 Hz, 2H), 5.75 (b,

10H), 4.24–3.63 (b, 32H), 2.25 (d, J = 7.5 Hz, 2H) ppm. HRMS (ESI) calcd for $C_{86}H_{82}F_{24}N_4O_{14}P_4$ $[M - 4PF_6 - 2H]^{2+,}$ m/z: 696.2835, found: 696.2830 $[M - 4PF_6 - 2H]^{2+}$.

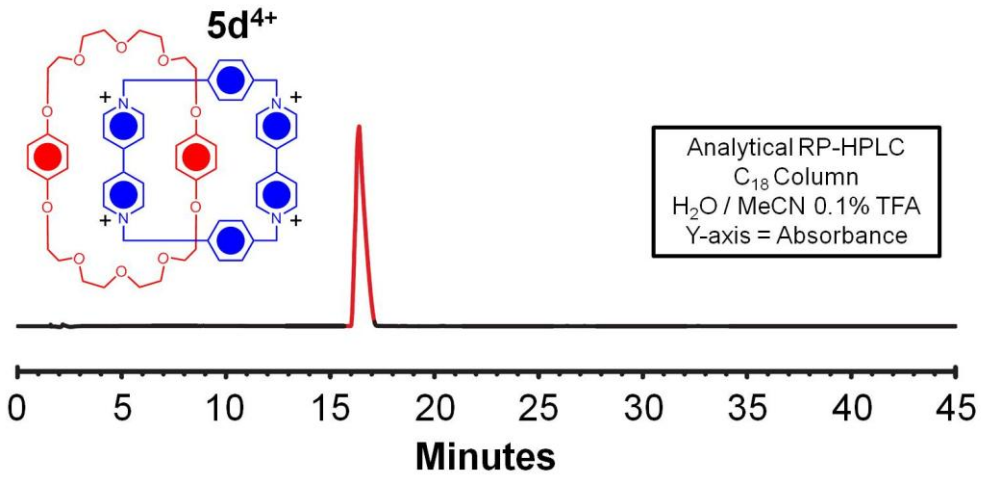

Figure S4. Analytical RP-HPLC of the pure catenane **5d**$^{4+}$; Abs @ 300 nm.

5d•4PF$_6$: Red solid (55 mg, 34%). ^{1}H NMR (500 MHz, CD_3CN, 298 K) δ = 8.86 (d, J = 7.1 Hz, 8H), 7.80 (s, 8H), 7.67 (d, J = 7.1 Hz, 8H), 6.17 (broad s, 4H), 3.98–3.82 (broad m, 16 H), 3.74 (broad m, 4H), 3.62 (broad m, 4H), 3.56 (broad m, 4H), 3.47 (broad s, 4H), 3.36 (broad m, 4H) ppm. LRMS (ESI) calcd for $C_{64}H_{72}F_{12}N_4O_{10}P_2$ $[M - 2PF_6]^{2+,}$ m/z: 673.3, found: 673.3 $[M - 2PF_6]^{2+}$.

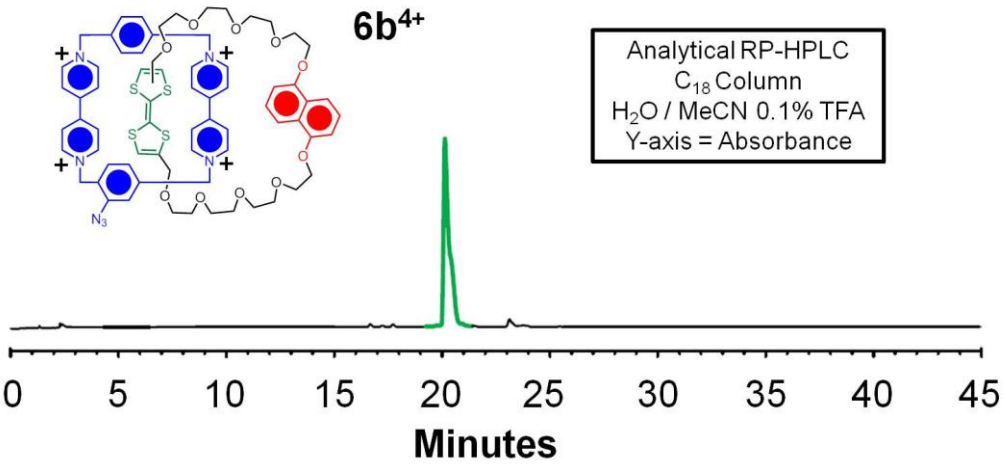

Figure S5. Analytical RP-HPLC of the pure catenane **6b**$^{4+}$; Abs @ 300 nm.

6b•4PF$_6$: Green solid (123 mg, 65%). ^{1}H NMR (500 MHz, CD_3CN, 298 K) δ = 9.14–8.42 (broad m, 8H), 7.89–7.18 (broad m, 13H), 6.83–6.55 (broad m, 2H), 6.17–5.97 (broad m, 2H), 5.95–5.28 (broad m, 8H), 4.38–3.44 (broad m, 36H) ppm. ^{13}C NMR (125 MHz, CD_3CN, 298 K) δ = 206.23, 153.51, 144.53, 130.36, 125.98, 125.70, 125.16, 125.05, 124.22, 113.48, 105.48, 105.40, 70.82, 70.54, 70.44, 70.24, 70.01, 69.66, 69.49, 69.32, 67.36, 64.05, 63.64, 29.56 ppm. HRMS (ESI) calcd for $C_{70}H_{75}F_{12}N_7O_{10}P_2S_4$ [M – 2PF$_6$]$^{2+}$, m/z: 795.6865, found: 795.6868 [M – 2PF$_6$]$^{2+}$.

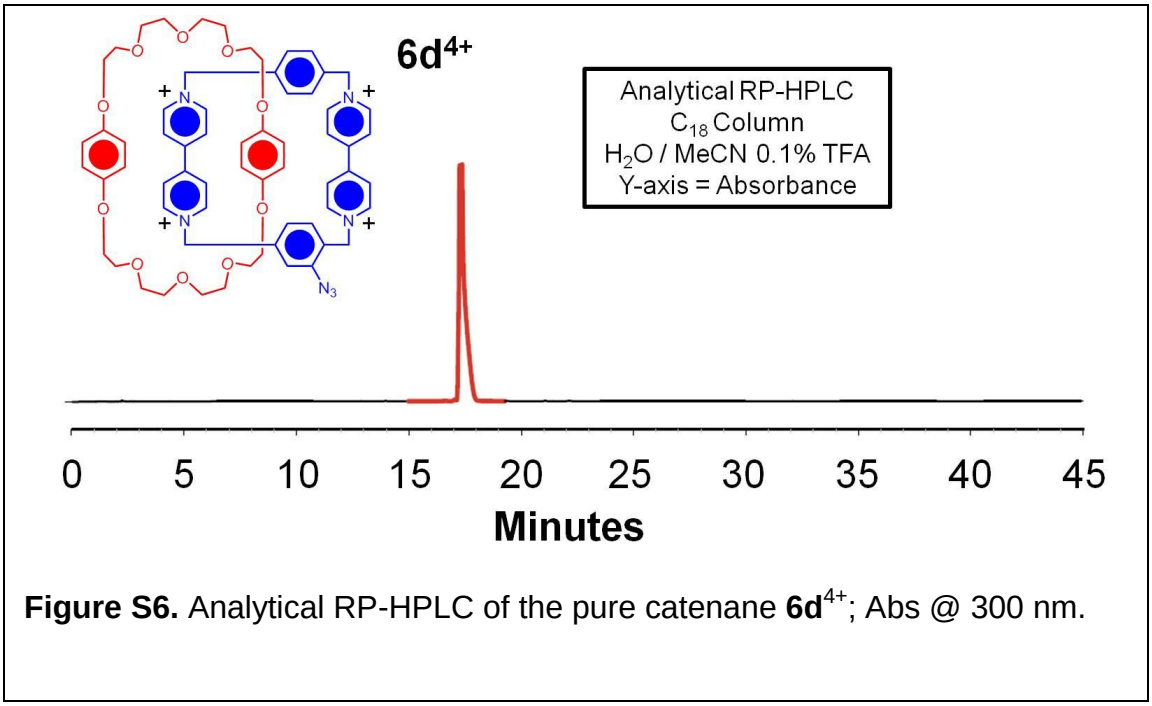

Figure S6. Analytical RP-HPLC of the pure catenane **6d**$^{4+}$; Abs @ 300 nm.

6d•4PF$_6$: Red solid (55 mg, 34%). ^{1}H NMR (500 MHz, CD_3CN, 298 K) δ = 8.90 (m, 8H), 7.90–7.57 (m, 15H), 6.18 (s, 4H), 5.69 (m, 8H), 4.01–3.52 (broad m, 32H), 3.56 (broad s, 4H) ppm. ^{13}C NMR (125 MHz, CD_3CN, 298 K) δ = 151.67, 149.69, 145.67, 145.42, 145.23, 144.57, 144.35, 144.25, 139.90, 138.10, 136.27, 136.24, 133.15, 130.53, 130.41, 126.68, 126.40, 125.20, 125.06, 124.99, 119.46, 114.60, 70.37, 70.05, 69.56, 69.43, 69.19,

68.71, 67.23, 66.24, 64.31, 63.81, 59.29 ppm. HRMS (ESI) calcd for $C_{64}H_{72}F_{17}N_6O_{12}P_3$ $[M - PF_6]^{+\cdot}$ *m/z*: 1532.415, found: 1532.419 $[M - PF_6]^+$.

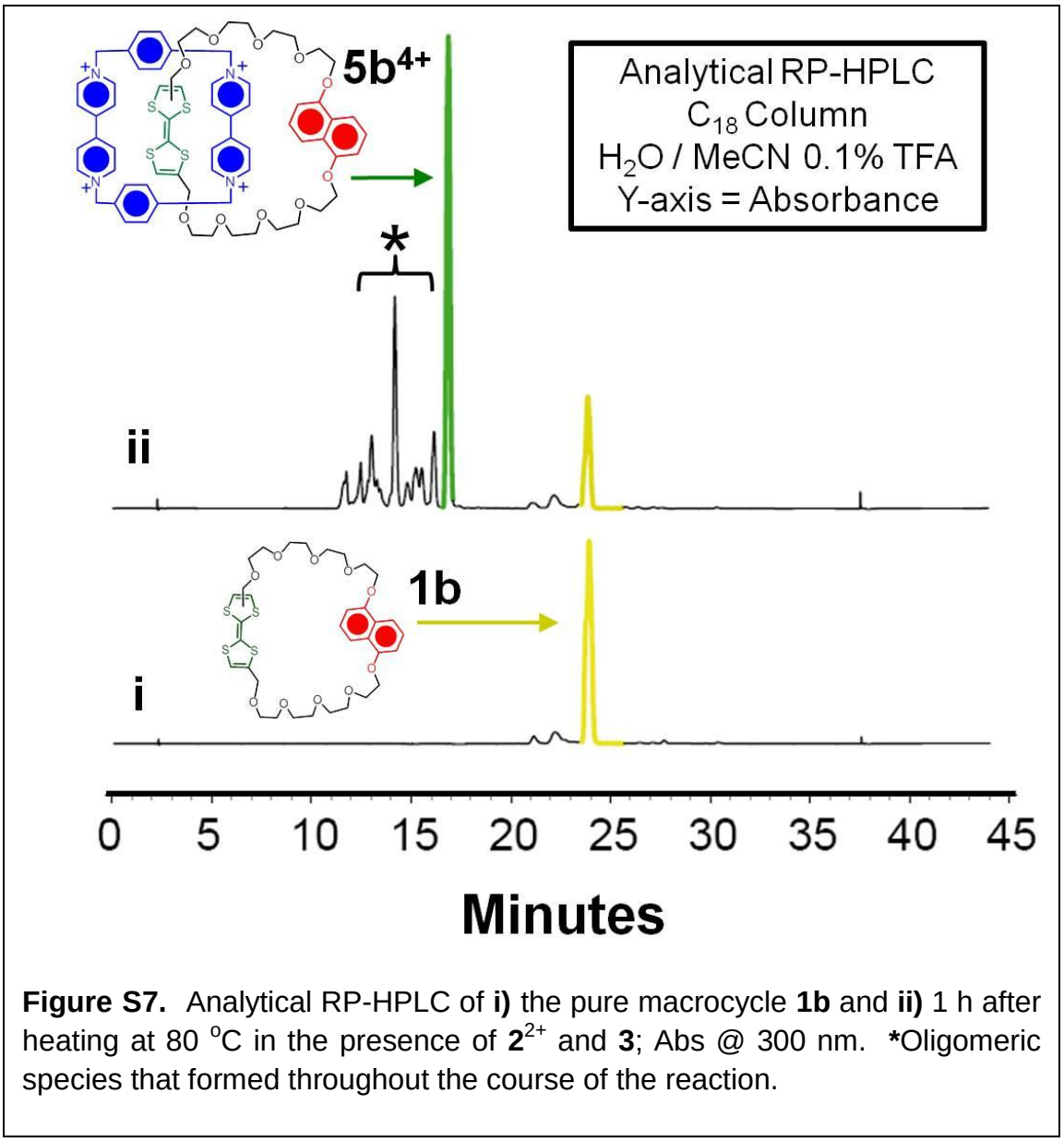

Figure S7. Analytical RP-HPLC of **i)** the pure macrocycle **1b** and **ii)** 1 h after heating at 80 °C in the presence of $\mathbf{2}^{2+}$ and **3**; Abs @ 300 nm. ***Oligomeric species that formed throughout the course of the reaction.

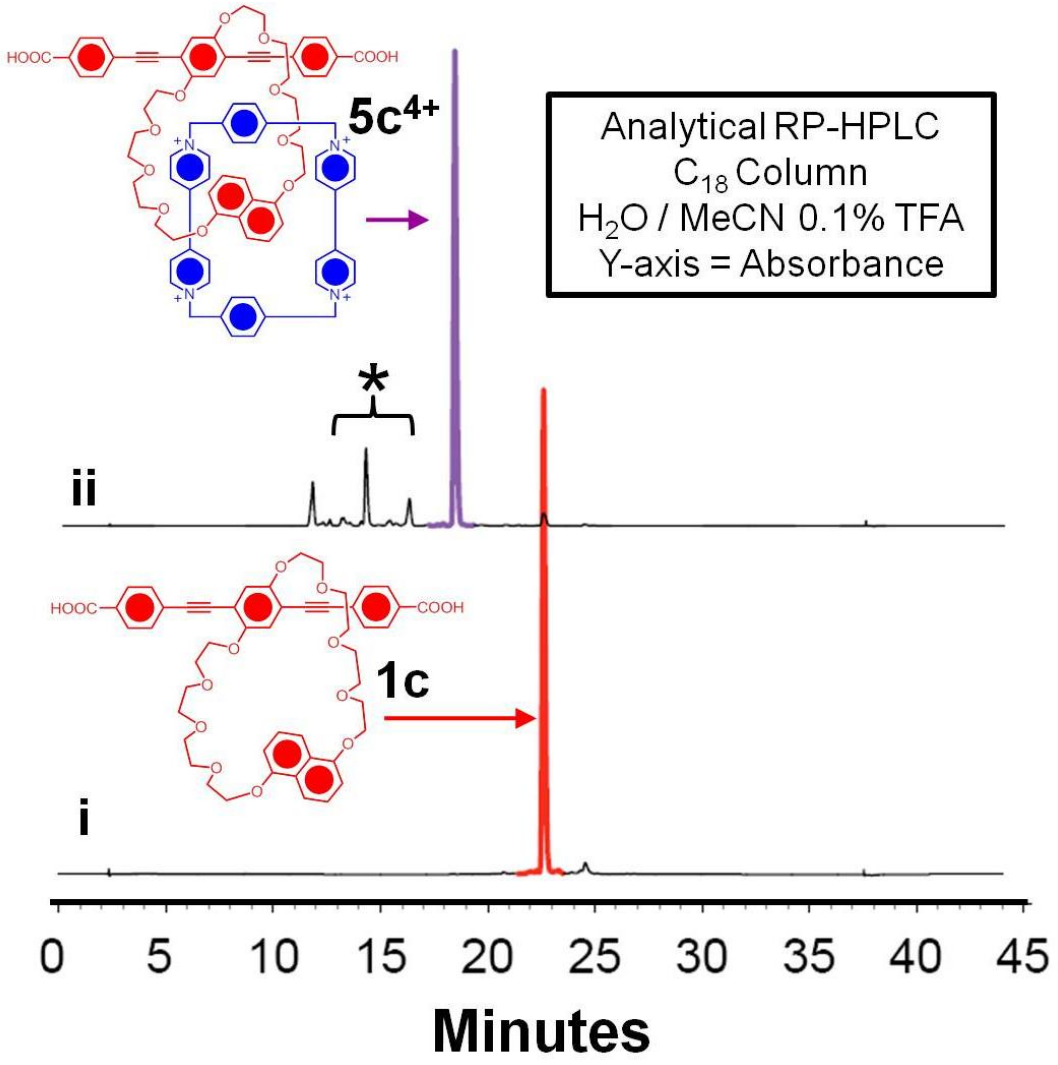

Figure S8. Analytical RP-HPLC of **i)** the pure macrocycle **1c** and **ii)** 1 h after heating at 80 ^{o}C in the presence of $\mathbf{2}^{2+}$ and **3**; Abs @ 300 nm. *****Oligomeric species that formed throughout the course of the reaction.

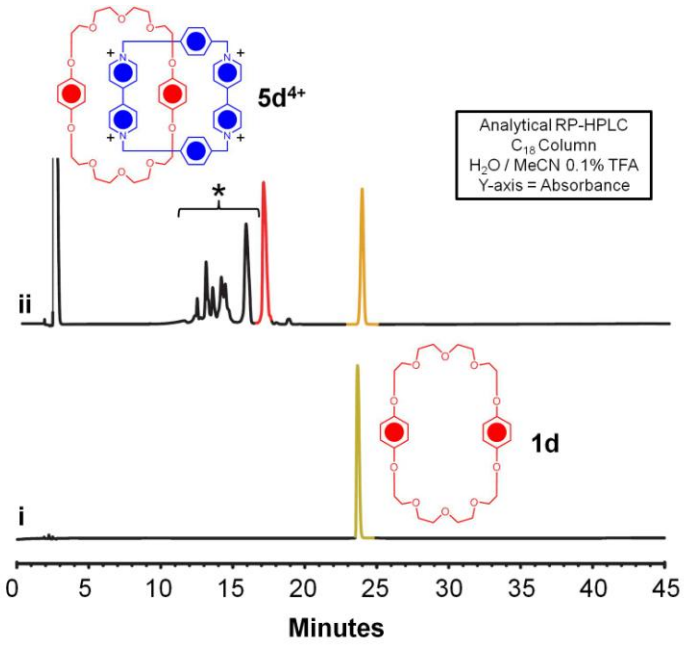

Figure S9. Analytical RP-HPLC of **i)** the pure macrocycle **1d** and **ii)** 1 h after heating at 80 ^{o}C in the presence of $\mathbf{2}^{2+}$ and **3**; Abs @ 300 nm. *****Oligomeric species that formed throughout the course of the reaction.

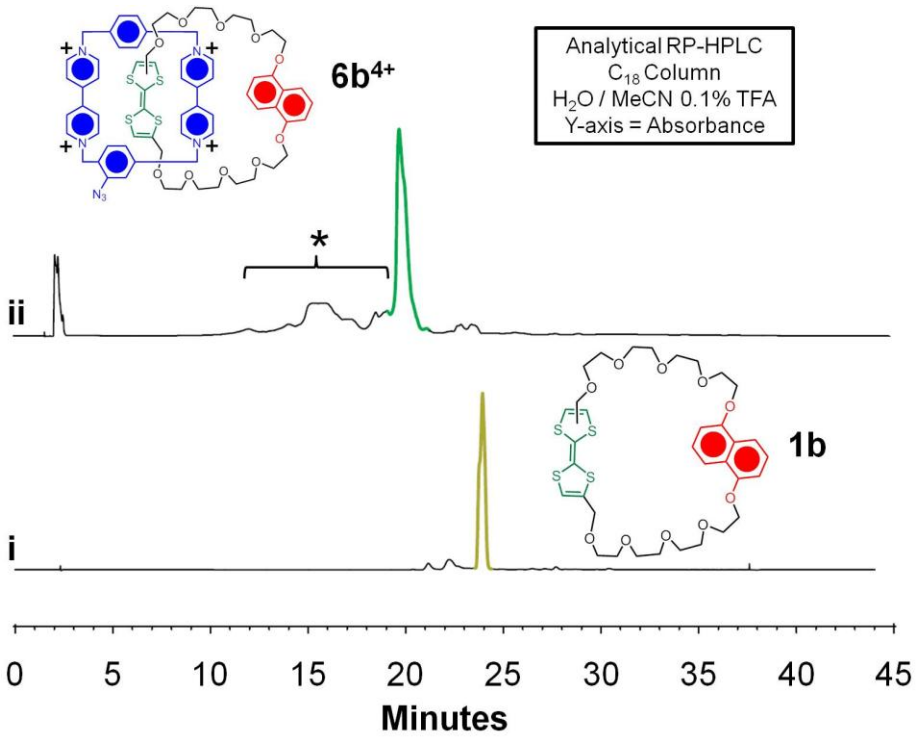

Figure S10. Analytical RP-HPLC of **i)** the pure macrocycle **1b** and **ii)** 1 h after heating at 80 ^{o}C in the presence of $\mathbf{2}^{2+}$ and **4**; Abs @ 300 nm. *****Oligomeric species that formed throughout the course of the reaction.

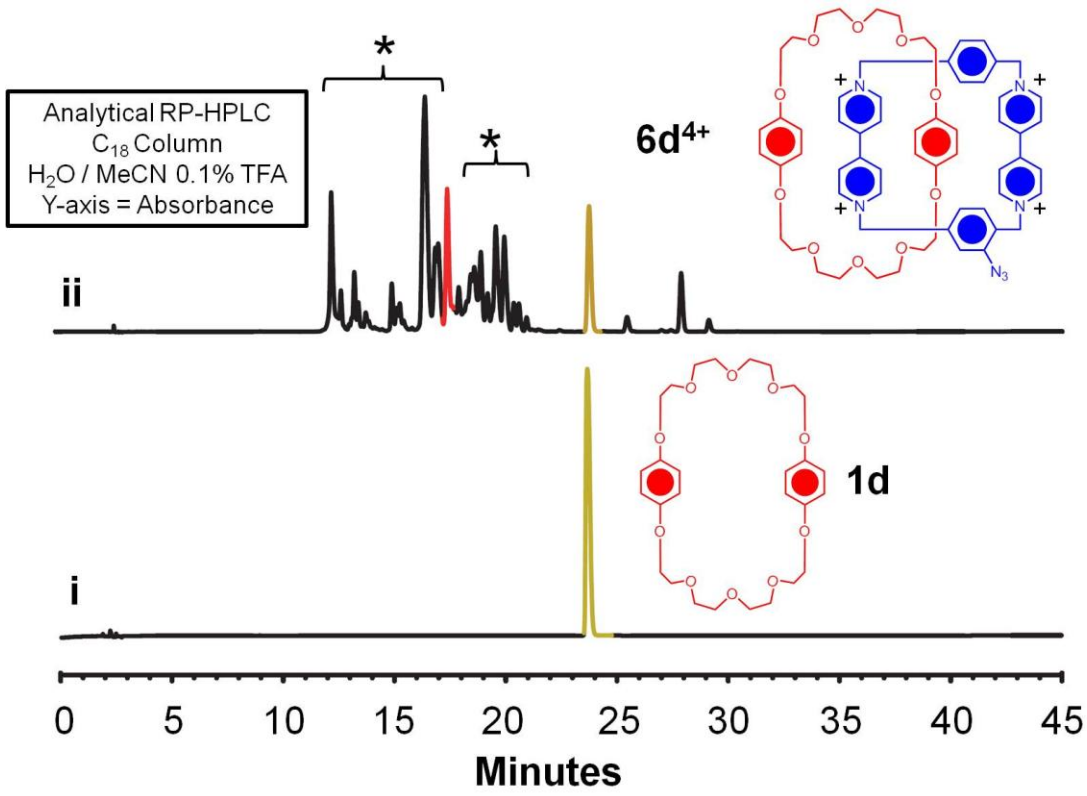

Figure S11. Analytical RP-HPLC of **i)** the pure macrocycle **1d** and **ii)** 1 h after heating at 80 ^{o}C in the presence of $\mathbf{2}^{2+}$ and **4**; Abs @ 300 nm. ***Oligomeric species that formed throughout the course of the reaction.

DB: A mixture of **S1** (300 mg, 0.37 mmol), 2,6-diisopropylphenol (400 mg, 2.2 mmol), and K_2CO_3 (500 mg, 3.6 mmol) was heated under reflux in MeCN (10 ml) for 18 h. After cooling to ambient temperature, the reaction mixture was added to water (50 ml) and extracted into CH_2Cl_2 (50 ml). The organic layers were dried ($MgSO_4$), filtered, concentrated under reduced pressure, and purified by flash column chromatography on SiO_2 (EtOAc:hexanes, 1:1 v/v) to afford the dumbbell **DB** as a viscous yellow liquid (73 mg, 24%). ^{1}H NMR (500 MHz, $CDCl_3$, 298K): δ = 7.86 (d, J = 8.5 Hz, 2H), 7.34 (t, J = 8.0 Hz, 2H), 7.1 (s, 6H), 6.84 (d, J = 7.5 Hz, 2H), 4.30 (t, J = 5.0 Hz, 4H), 4.01 (t, J = 5.0

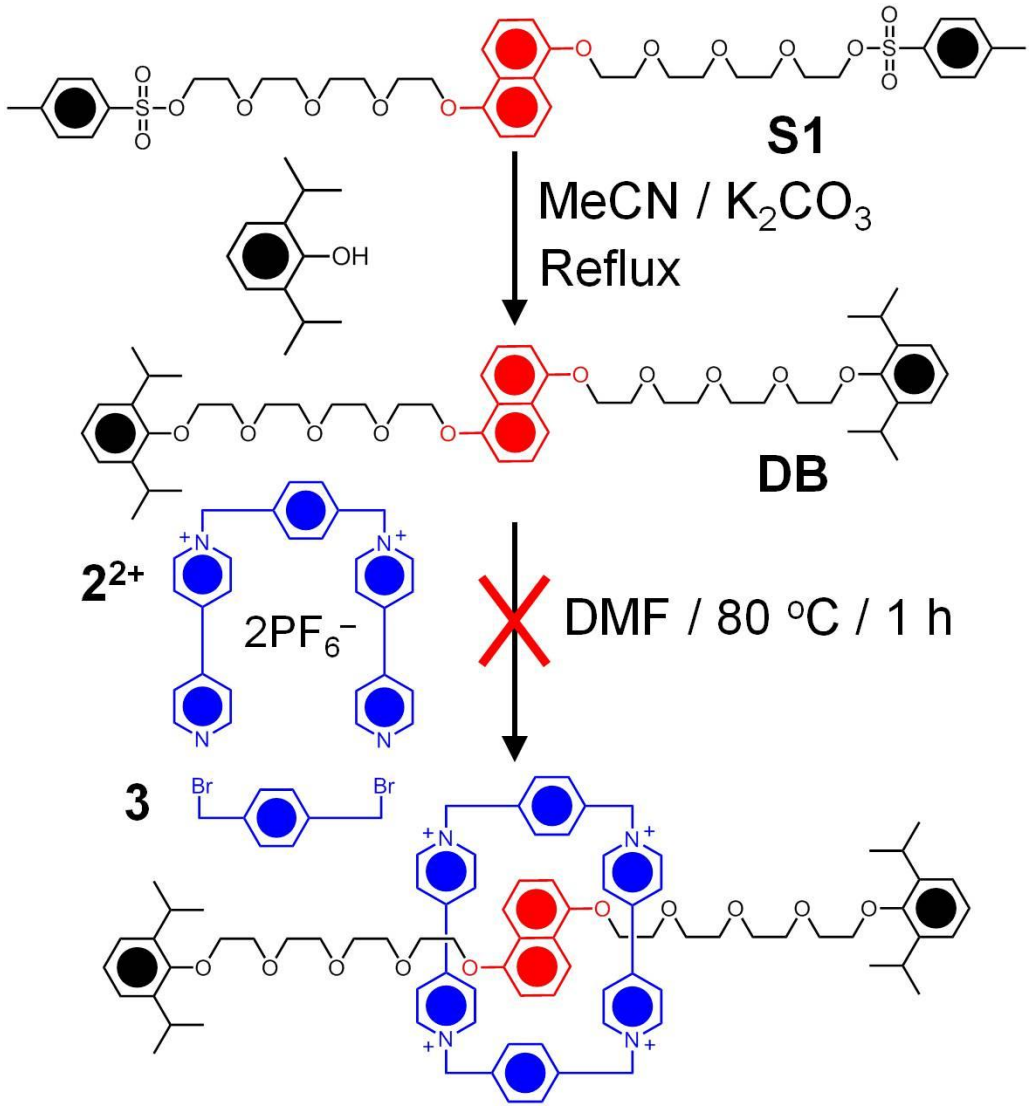

Scheme S1. Synthesis of the dumbbell **DB** and the attempted synthesis of the [2]rotaxane employing identical reactions conditions as the [2]catenanes.

Hz, 4H), 3.92–3.90 (m, 4H), 3.87–3.82 (m, 8H), 3.79–3.74 (m, 12H), 3.39 (hept, J = 7.0 Hz, 4H), 1.22 (d, J = 7.0 Hz, 24H) ppm. ^{13}C NMR (125 MHz, $CDCl_3$, 298K): δ = 154.3, 153.0, 141.8, 127.8, 125.0, 124.6, 124.0, 114.6, 105.6, 73.8, 71.0, 71.0, 70.8, 70.7, 70.5, 69.8, 67.8, 26.2, 24.1 ppm. LRMS (ESI) calcd for $C_{50}H_{73}O_{10}$ $[M + H^+]^+$, m/z: 833.5, found: 833.5 $[M + H^+]^+$.

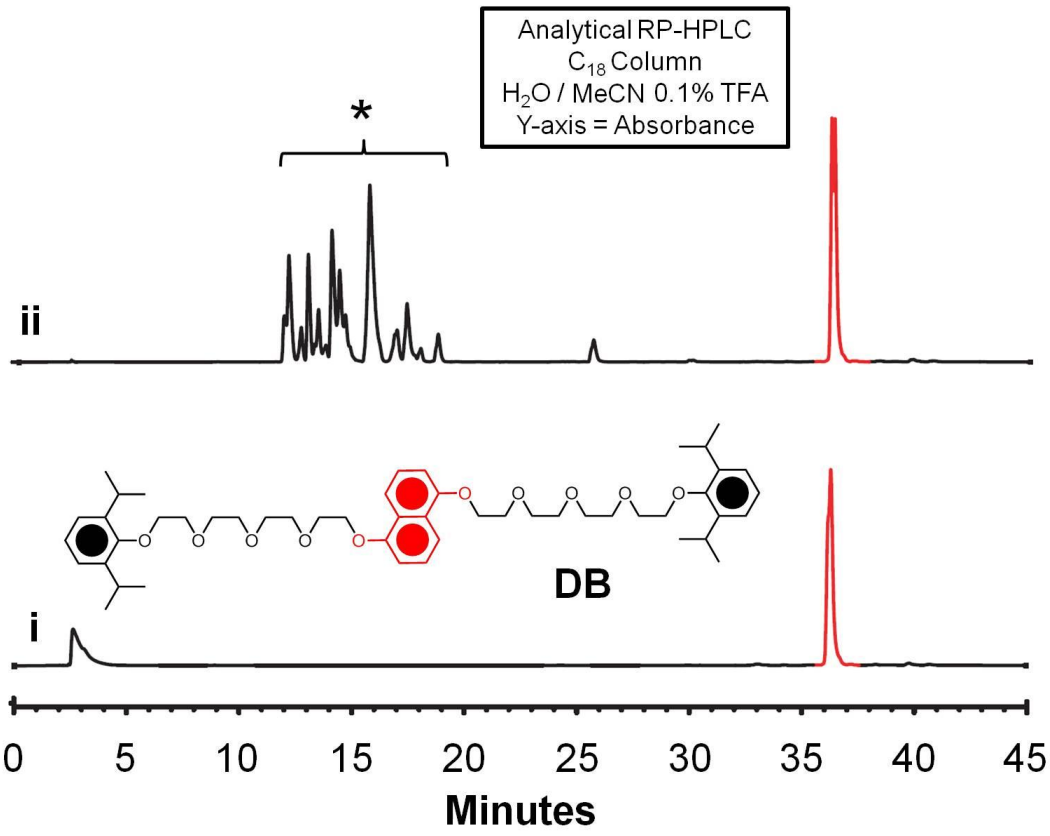

Figure S12. Analytical RP-HPLC of **i)** the pure dumbbell **DB** and **ii)** 1 h after heating at 80 ^{o}C in the presence of $\mathbf{2}^{2+}$ and **3**; Abs @ 300 nm. ***Oligomeric species that formed throughout the course of the reaction. The target [2]rotaxane was not able to be isolated from the reaction mixture.

3. X-Ray Crystallography

Single crystals of **6b•4PF$_6$** and **6d•4PF$_6$** suitable for single-crystal X-ray crystallography were both grown by slow-vapor diffusion of *i*Pr$_2$O into individual MeCN solutions of the catenanes at 298 K. After a week, large crystals were observed and used subsequently for structural determination.

Crystal data for **6b•4PF$_6$**: $C_{34}H_{39}O_{10}S_4$, $C_{36}H_{30}N_7$, 4(PF_6), 3(C_2H_3N), M_r = 1999.60, triclinic, $P\bar{1}$, a = 13.6925(4), b = 14.1263(4), c = 28.1027(9) Å, α = 96.491(2), β = 103.206(2) ɣ = 107.826(2)°. V = 4938.8(3) Å^3, T = 100(2) K, Z = 2, D_c = 1.345 g cm^{-3}, μ(Cu-K$_\alpha$) = 2.389 mm^{-1}, F (000) = 2048. Independent measured reflections 37696. R_1 = 0.1181, wR_2 = 0.3394 for 15377 independent observed reflections [$2\theta \leq 124.6°$, $I > 2\sigma(I)$]. CCDC 887695. The SQUEEZE program was used to remove contributions of disordered solvent molecules from the unit cell.

Crystal data for **6d•4PF$_6$**: $C_{36}H_{31}N_7$, $C_{28}H_{40}O_{10}$, 4(F_6P), 5(C_2H_3N), M_r = 1883.43, triclinic, P_1, a = 13.5802(6), b = 13.7732(6), c = 26.2234(11) Å, α = 87.017(3), β = 81.927(3) ɣ = 60.811(2)°. V = 4238.9(3) Å^3, T = 100(2) K, Z = 2, D_c = 1.476 g cm^{-3}, μ(Cu-K$_\alpha$) = 0.205 mm^{-1}, F (000) = 1940. Independent measured reflections 99182. R_1 = 0.1198, wR_2 = 0.3430 for 24299 independent observed reflections [$2\theta \leq 124.6°$, $I > 2\sigma(I)$]. CCDC 887694.

In the case of both **6b**$^{4+}$ and **6d**$^{4+}$, the X-ray structures reveal (Figure S13) that the azide groups do not significantly disrupt the noncovalent bonding interactions in comparison to their unfunctionalised derivatives **5b**$^{4+}$ and **5d**$^{4+}$. In particular, neither the donor-acceptor [π•••π] interactions or the [C–H•••O] bonding between the alpha protons of the encircled BIPY^{2+} unit and some of the oxygen atoms of the macrocylic polyether are not observed to vary by more than a few tenths of an angstrom. These X-ray structures support the hypothesis that the azide group does not interrupt these noncovalent bonding interactions during the template-directed synthesis, and so as a consequence, the yields do not suffer.

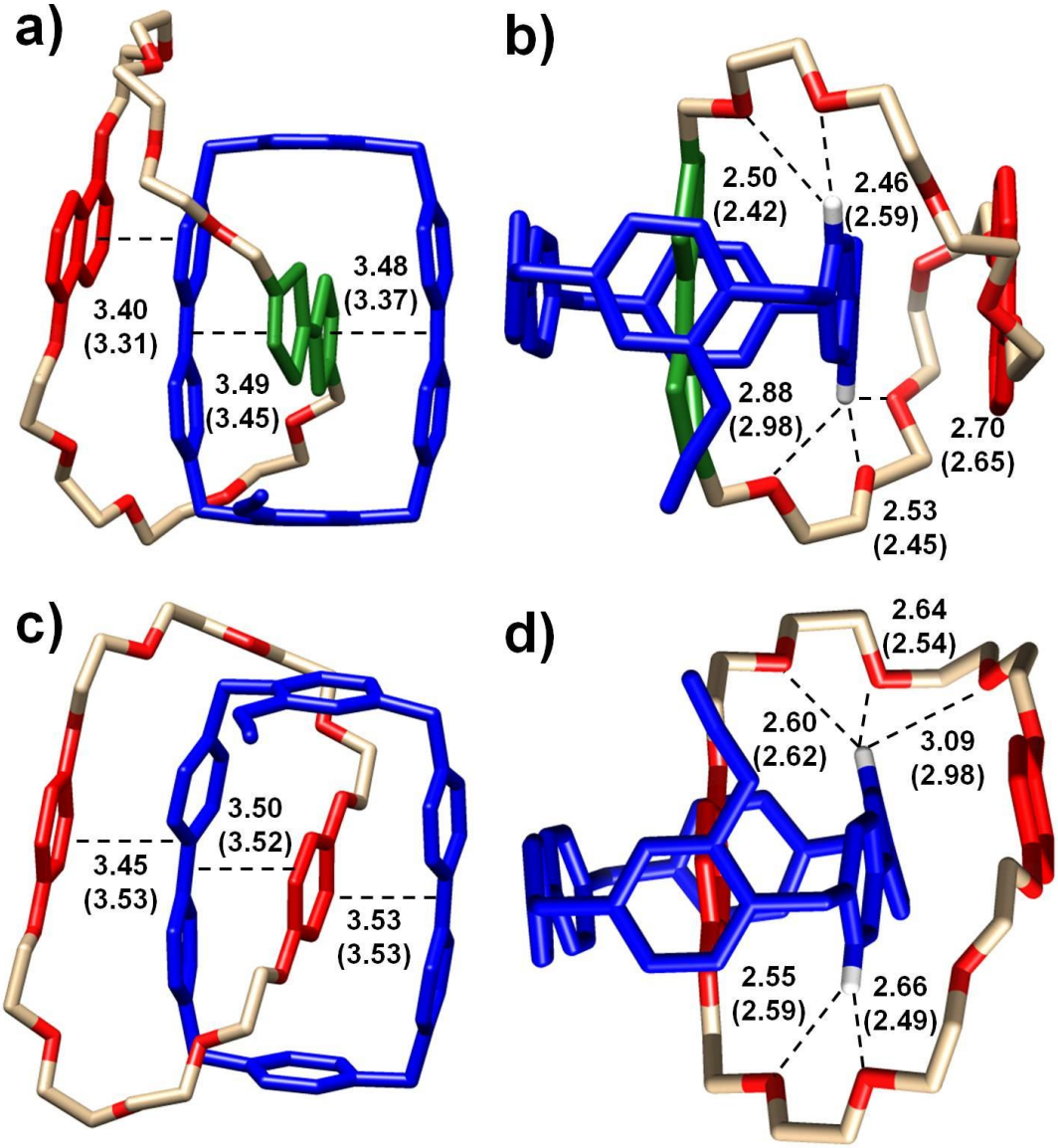

Figure S13. The X-ray crystal structures of **6b**$^{4+}$ and **6d**$^{4+}$ elucidating the donor-acceptor [π•••π] interactions and [C–H•••O] bonding. All dashed lines are a measure of distances in Angstroms. The values in parentheses correspond to the distances measured in X-ray structures of the unfunctionalised analogues **5b**$^{4+}$ and **5d**$^{4+}$.

4. References

S1 C. J. Bruns, S. Basu, and J. F. Stoddart, *Tetrahedron Lett.,* 2010, **51**, 983–986.

S2 M. Asakawa, P. R. Ashton, V. Balzani, A. Credi, C. Hamers, G. Mattersteig, M. Montalti, A. N. Shipway, N. Spencer, J. F. Stoddart, M. S. Tolley, M. Venturi, A. J. P. White, and D. J. Williams, *Angew. Chem. Int. Ed.,* 1998, **37**, 333–337.

S3 Y.-L. Zhao, L. Liu, W. Zhang, C.-H. Sue, Q. Li, O. Š. Miljanic, O. M. Yaghi, and J. F. Stoddart, *Chem. Eur. J.,* 2009, **13**, 13356–13380.

S4 B. L. Allwood, N. Spencer, H. Shahriari-Zavareh, J. F. Stoddart and D. J. Williams, *J. Chem. Soc., Chem. Commun.,* 1987, 1061–1064.

S5 B. Odell, M. V. Reddington, A. M. Z. Slawin, N. Spencer, J. F. Stoddart, and D. J. Williams, *Angew. Chem. Int. Ed. Engl.,* 1988, **27**, 1547–1550.

S6 M. A. Olson, A. Coskun, R. Klajn, L. Fang, S. K. Dey, K. P. Browne, B. A. Grzybowski, and J. F. Stoddart, *Nano Lett.,* 2009, **9**, 3185–3190.